Available online at www.sciencedirect.com

ScienceDirect

Procedia CIRP 99 (2021) 375–380

www.elsevier.com/locate/procedia

14th CIRP Conference on Intelligent Computation in Manufacturing Engineering, CIRP ICME '20

Buckling behavior of 3D printed composite isogrid structures

Daniele Ciccarelli[a], Archimede Forcellese[a], Luciano Greco[a], Tommaso Mancia[a], Massimiliano Pieralisi[a], Michela Simoncini[b*], Alessio Vita[a]

[a]*Università Politecnica delle Marche, Via Brecce Bianche, Ancona 6011, Italy*
[b]*Università Telematica eCampus, Via Isimbardi 10, Novedrate 22060, Italy*

* Corresponding author. Tel.: +39 071 2204443. *E-mail address:* michela.simoncini@uniecampus.it; m.simoncini@staff.univpm.it

Abstract

Different 3D printed composite isogrid structures in polyamide reinforced with 20% in weight of short carbon fiber were manufactured by means of fused deposition modeling process. Six configurations were realized varying the rib width and the rib thickness of the structures. The isogrid panels were tested under compressive load in order to investigate the effect of geometric parameters on the buckling behavior, in terms of strength and specific strength. Different failure modes were identified, depending on geometric parameters: global and local buckling. Finally, optical microscopy was carried out in order to analyze the fractured ribs after buckling. It was demonstrated that the configurations which result in the highest strength are not the same of those providing the highest specific strength.

Peer-review under responsibility of the scientific committee of the 14th CIRP Conference on Intelligent Computation in Manufacturing Engineering, 15-17 July 2020.

Keywords: Composite materials; 3D printing; Isogrid structures

1. Introduction

Automotive industry is facing new challenges arising from the necessity of reducing car weight while ensuring high components performances. More and more stringent regulations on fuel consumption and efficiency are forcing engineers in developing new materials and manufacturing methods in order to enhance specific strength and specific resistance of the structures [1]. In addition, the adoption of eco-friendly materials and processes represents a key aspect to fulfill the requirements of regulatory frameworks [2]. As far as the development of new materials is concerned, the industrial and academic researches concentrated on composite materials. In particular, in the 90′s research focused on discontinuously reinforced metal matrix composites since the final component can be shaped using conventional metal forming operations [3,4]. In the last years, the interest mainly focused on Carbon Fiber Reinforced Polymers (CFRPs) due to the development of automated fiber placement processes, which allowed to overcome the drawbacks typical of manual operations in terms of productivity and repeatability of the mechanical properties of composite laminates [5–7]. The final assembly can be obtained by means of both adhesive bonding [8] and mechanical fastening [9,10].

In this context, a rapid evolution in the design of some components, especially those subjected to compressive loads, led to developing of new structures which allowed to strongly reduce weights, although maintaining high mechanical properties. To this purpose, isogrid structures, realized by manufacturing stiffeners in the form of equilateral triangles attached to sheets, are used for providing stiffness and resistance to compression-loaded components [11].

Isogrid structures were developed by the McDonnell-Douglas Corporation in the 60's. They were machined from a single piece of aluminum alloy and were used in different aircrafts [12]. Unfortunately, the manufacturing of isogrid structures in aluminum alloy was an expensive process, characterized both by long manufacturing time and a large amount of material waste. Recently, the diffusion of CFRPs, realized using an additive approach in their manufacturing processes, led to the development of isogrid structures in composite materials, characterized by higher performances and

Peer-review under responsibility of the scientific committee of the 14th CIRP Conference on Intelligent Computation in Manufacturing Engineering, 15-17 July 2020.
10.1016/j.procir.2021.03.053

efficiency than those provided by isogrid structures in aluminum alloys [13].

The typical failure mode of compressive-loaded isogrid structures is buckling, which can occur in two different modes: global and local buckling [13]. The global buckling occurs as the whole structure collapses, whilst the local buckling involves the local failure of ribs. This different failure mode is related to the geometric parameters of isogrid structure, such as cell height, rib width, rib height, rib thickness, winding angle (in case of cylindrical structures) and skin thickness.

Many investigations are related to the optimization of such parameters in order to maximize the permissible buckling load of isogrid structures [14–17]. However, most of them concerned the study of cylindrical isogrid structures due to the large applications in the aeronautical sector. Only few researches refer to flat isogrid panels, demonstrating that an in-depth study of this topic is necessary. Totaro demonstrated that for composite isogrid panels, local and global buckling were the predominant failure modes, and he developed analytical model to minimize panel weight [18]. Shroff et al. predicted the damage of isogrid panels using a proper failure model [19].

As far as manufacturing processes are concerned, one of the most promising techniques for the production of high quality and low-cost composite parts is 3D printing. Indeed, this process has experienced an accelerated development in the last ten years, allowing the manufacturing of composite components with higher mechanical properties than those realized in aluminum alloys. The most used 3D printing method is Fused Deposition Modeling (FDM) due to its economic affordability and reliability. Typically, composites FDM process is performed by extruding a thermoplastic filament filled with short carbon fibers even tough long reinforcements are gaining market share [20].

FDM 3D printing can represent a valid method for the manufacturing of isogrid structures in CFRP, especially when the reduction of manufacturing time and costs is predominant with respect to product performances. However, this topic is not sufficiently investigated in literature, since only a previous paper of the authors is available [21]. In that work, it was demonstrated that failure of the 3D printed composite isogrid structures during compression test is due to the global buckling failure mode; furthermore, the rise in cell height results in a decrease in both maximum load and specific maximum load whilst the rise in rib width leads to an increase in both peak load and specific maximum load. Li et al. investigated the mechanical behavior of 3D printed lattice isogrid structure through compression tests and finite element method analysis in order to investigate the different failure modes of the structures [22].

In this context, the effect of geometric parameters on the mechanical behavior of 3D printed composite isogrid structures requires a more detailed investigation in order to define a failure mode map as a function of geometric parameters which can be used for the optimal design of the isogrid structures. To this purpose, in this paper, different isogrid panels were manufactured by FDM 3D printing by exploiting carbon fiber reinforced polyamide. The structures, realized with different rib widths and rib thicknesses, were tested under compression load. The effect of geometric parameters on maximum load, specific maximum load and buckling failure modes were investigated. Optical microscopy analysis was also carried out in order to observe the fractured ribs after buckling.

2. Fabrication and testing

2.1. 3D printing process

An FDM 3D printer, produced by Roboze spa, was used to manufacture composite isogrid panels (Fig. 1). It is characterized by a nozzle of 0.6 mm and an average printing speed of 50 mm/s. The composite material used is a polyamide reinforced with short carbon fibers at 20% in weight (commercial name: CarbonPA). According to the material technical datasheet, the elastic modulus (E) and the ultimate tensile strength (UTS) of the CarbonPA are 15.5 GPa and 138 MPa, respectively.

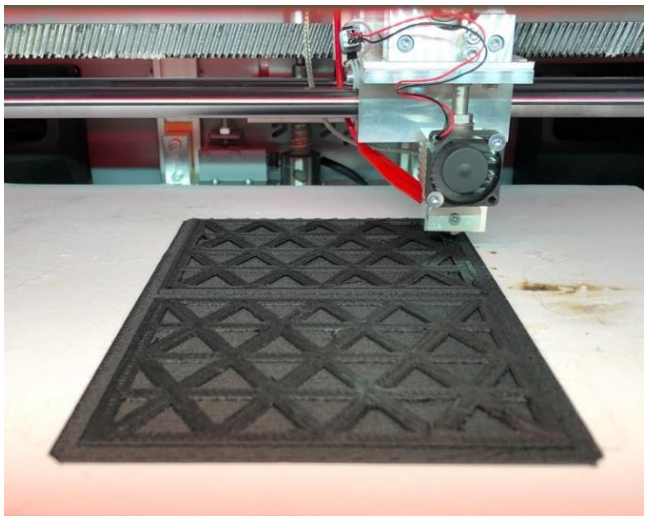

Fig. 1. 3D printing process of composite isogrid panels.

Since polyamide is subjected to moisture adsorption which causes a strong decrease in the mechanical performances, before printing, the spool containing the composite filament was dried for 4 hours at 120°C. Moreover, during the printing phase it was maintained at 70°C to avoid humidity adsorption. Filament extrusion was executed at a temperature higher than the glass transition temperature (Tg) of polyamide. Linear internal infill pattern was chosen for the manufacturing of isogrid panels due to its elevated resistance (Fig. 2).

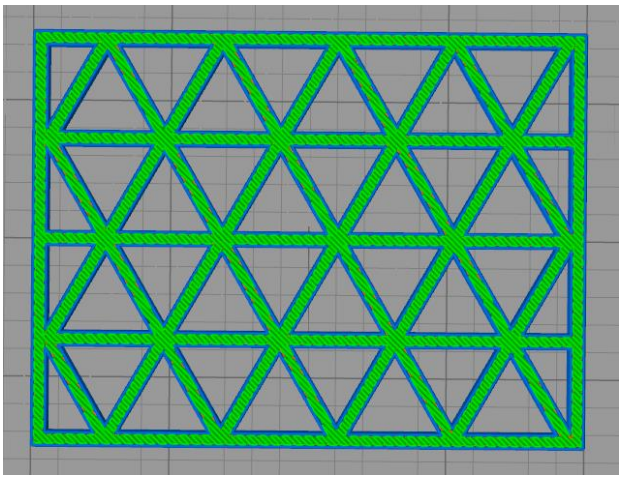

Fig. 2. Slicing of an isogrid panel during pre-processing.

2.2. Design parameters of isogrid structures

A CAD software, able to export .STL files, was used to design isogrid structures. The mesh file was imported in a slicing software able to create a .GCODE file for translating the 3D model into instructions for the 3D printer.

A total of 18 isogrid structures, realized in six different configurations, were manufactured. Fig. 3 shows a typical isogrid structure, characterized by three geometric parameters: rib width (x), rib thickness (z) and cell height (t). However, in the present study, the cell height value was kept constant. Table 1 reports the values of geometric parameters investigated in the present work.

In order to maintain the unsupported length of the structure (as defined in the Euler's critical load formula) unchanged, the size of the sides parallel and perpendicular to the longitudinal ribs was kept constant, with values of 106 and 80 mm, respectively.

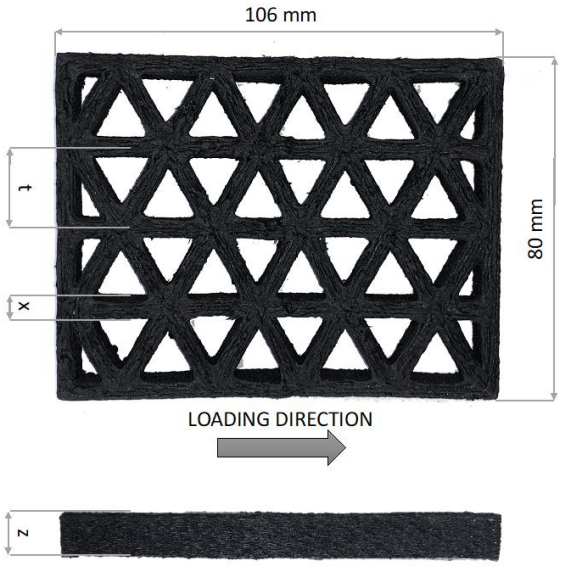

Fig. 3. Geometric parameters of the isogrid structures.

Table 1. Geometric parameters and weight of the isogrid structures.

Rib width, x [mm]	Rib thickness, z [mm]	Cell height, t [mm]	Weight, w [g]
3	8	18	43.3
3	10	18	54.9
3	15	18	81.9
5	8	18	68.2
5	10	18	98.6
5	15	18	127.3

In order to avoid moisture adsorption, after printing process, isogrid structures were subjected to a cooling phase at room temperature in a controlled environment for 2 hours. Then, they were weighted by means of an analytical balance. Table 1 also shows the weights of each isogrid structure.

2.3. Compression tests

A universal testing machine was used to perform compression test. Slow platen speed was chosen (0.5 mm/min) in order to avoid undesired inflection of the structures. During buckling test, load (P) and displacement (Δh) were acquired. Moreover, in order to investigate the specific resistance, the ratio between the peak load (Pmax) and the weight (w) was considered. Video recording was also performed to identify the onset of the buckling phenomena.

3. Results and discussion

Results of buckling tests performed on 3D printed composite isogrid structures demonstrated the occurrence of both global and local buckling failure modes.

Fig. 4a shows an isogrid structure failed because of the occurrence of the global buckling; this failure mode occurs in isogrid panel characterized by relatively small rib thickness and involves the whole structure. Fig. 4b shows an isogrid panel collapsed due to the local buckling, occurred as the structures presents small values of rib width, involving only the ribs. In particular, under the geometric parameters investigated in the present work, local buckling failure mode occurs as the rib thickness is equal to 15 mm.

In order to observe the fractured isogrid structures after buckling tests, optical microscopy investigation was performed. Fig. 5 shows an isogrid structure fractured at a nodal intersection owing to the instability of the whole structure, leading to the collapse of the panel. On the contrary, Fig. 5b shows a magnification of a fractured rib of an isogrid structure failed due to the occurrence of local buckling, during which the crack propagation arises along the direction perpendicular to that of the compressive load. Such phenomenon happens as the structure slenderness is lower than that of the ribs.

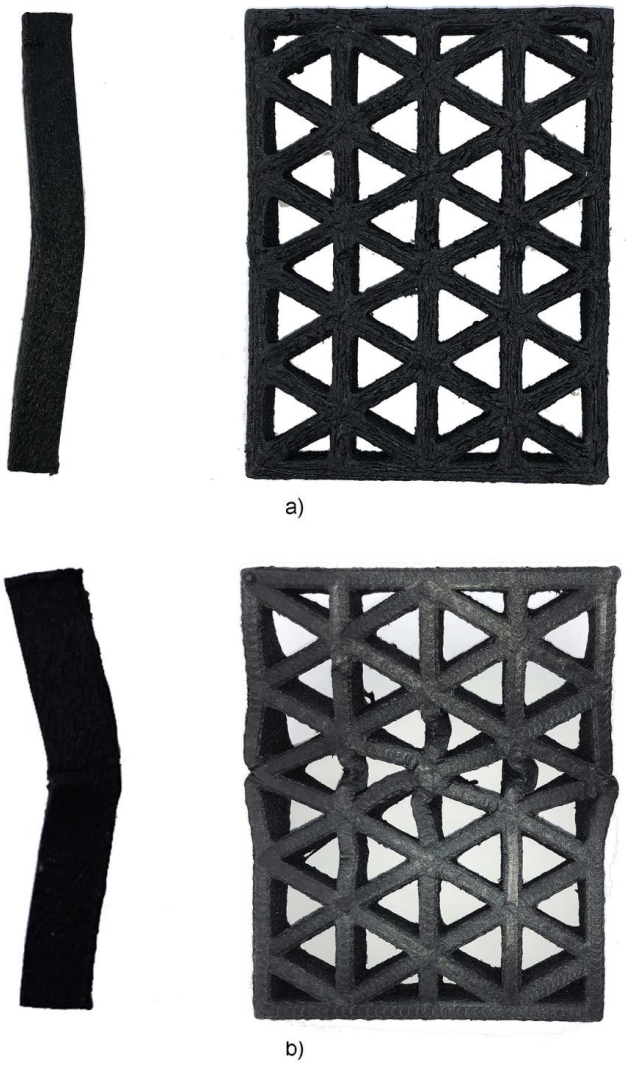

Fig. 4. (a) Global and (b) local buckling failure modes of 3D printed isogrid structures in CarbonPA.

Fig. 6 shows the P-Δh curves of the tested isogrid at different geometric parameters. It can be observed that the maximum load increases with rib thickness. As a matter of fact, for x=3 mm, the Pmax value increases by 54% as z rises from 8 to 10 mm, and by 56% as rib thickness further increases from 10 to 15 mm. A similar behavior can be seen in the isogrid structures characterized by a rib width of 5 mm, in which an increase in Pmax equal to 80% can be measured as z rises from 8 to 10 mm, and a further increase of about 31% as z passes from 10 to 15 mm. Moreover, Fig. 6 also shows that, for a given value of rib thickness, the increase in rib width leads to a remarkable rise in the resistance of the isogrid structures. In particular, as the x ranges from 3 to 5 mm, the enhance in Pmax is equal to 46% for z=8 mm, 71% for z=10 mm and 43% for z=15 mm.

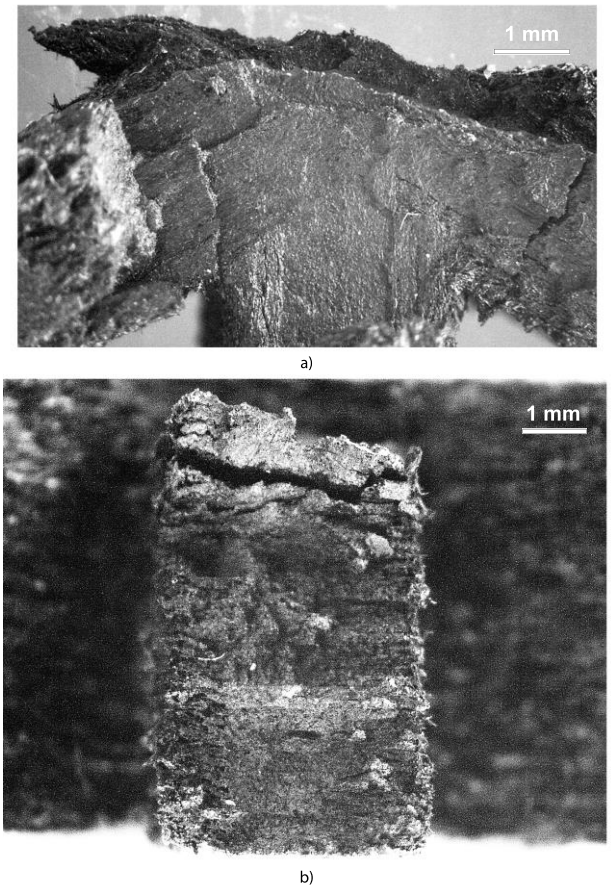

Fig. 5. Fracture surface magnification of: (a) global buckling failed isogrid structure (x = 3 mm, z= 8 mm, t=18mm), and (b) local buckling failed isogrid structure (x = 5 mm, z= 15 mm, t=18mm).

However, as far as the specific strength is concerned, different considerations can be drawn from the analysis of buckling tests results. In Fig. 7, the different configurations of the investigated isogrid structures are reported in terms of peak load and peak load to weight ratio.

As reported above, the maximum load is highly influenced by the geometric parameters of the structure whilst the Pmax/w values demonstrate a more uniform behavior. However, it can be observed that, irrespective of the z value taken into account, the composite isogrid structures with a rib width of 3 mm are characterized by a higher Pmax/w value than the structures with a x value of 5 mm. Moreover, similarly to the effect of the rib thickness on the maximum load, for a given rib width and cell height, the increase in z value leads to an increase in the specific strength. By analyzing Table 2, which summarizes the Pmax and Pmax/w values and reports the failure mode of the isogrid structures, it can be seen that the thicker isogrid configurations, characterized by the occurrence of the local buckling, exhibit a lower growth rate of specific strength. As a matter of fact, for x=3 mm, the specific strength increases of about 15.5% as z value rises from 8 to 10 mm, whilst an increase in Pmax/w of 8% can be obtained as rib thickness passes from 10 to 15 mm. As the rib width is equal to 5 mm, the Pmax/w increases of 28.5% and of 2.8% as the rib thickness increases from 8 to 10 mm and from 10 to 15 mm, respectively.

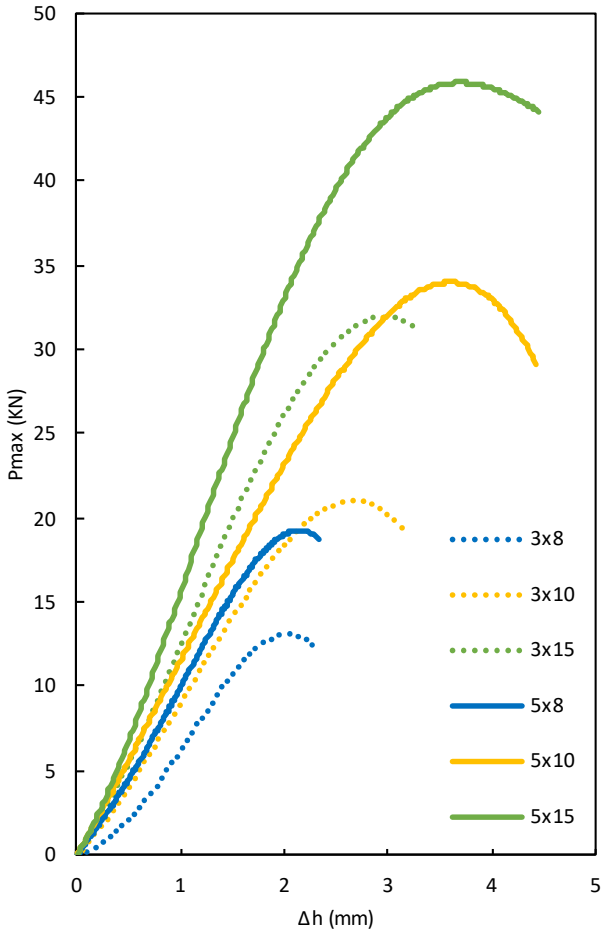

Fig. 6. Effect of geometric parameters on the peak load vs. displacement curves of the isogrid structures in Carbon PA (t=18 mm).

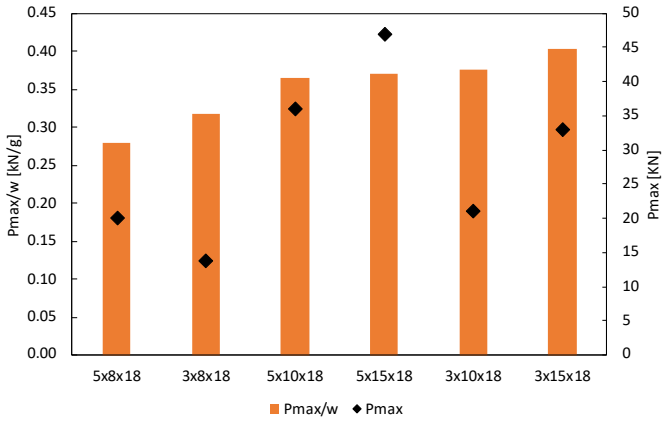

Fig. 7. Pmax and Pmax/w of the tested composite isogrid structures.

Finally, a significant aspect to consider during the design process of stiffened lattice structures concerns the possibility to develop structures characterized by different maximum load before failure but similar specific strength values, as shown in Fig. 7 and reported in Table 2.

Table 2: Maximum load, specific maximum load and buckling failure mode of the tested structures.

Isogrid Structure	Maximum Load [KN]	Specific Maximum Load [KN/g]	Buckling Failure Mode
3x8x18	13.7	0.32	Global
3x10x18	21.1	0.37	Global
3x15x18	33.0	0.40	Local
5x8x18	20.0	0.28	Global
5x10x18	36.1	0.36	Global
5x15x18	47.2	0.37	Local

4. Conclusion

In the present paper, 3D printed composite isogrid structures were realized and tested under compressive load. A polyamide reinforced with 20% in weight of short carbon fiber were exploited in FDM printing process to manufacture the structures. A total of six different configurations were tested under compressive load in order to investigate the effects of rib width and rib thickness on the strength and on the specific strength. The main outcomes can be summarized as follows:

- The increase in rib width leads to an increase in strength and to a decrease in specific strength;
- The rise in rib thickness results in an enhance in both strength and specific strength, even though such effect is less marked as the specific strength is taken into account;
- The isogrid structures can fail under local or global buckling, depending on geometric parameters;
- Structures configurations which lead to the highest strength are different to those resulting in the highest specific strength;
- Isogrid structures which undergo to local buckling failure mode demonstrate lower specific strength than expected.

In the light of these results, composite 3D printing demonstrates the capability of producing high performing isogrid panels. This can pave the way for a wide diffusion of this manufacturing method in sector such as aerospace for the production of structural components.

Future work will be focused in the correlation of cell height effect on the mechanical performances of the structures, taking into account also moisture adsorption of the polyamide.

Acknowledgments

This research was founded by POR FESR Abruzzo 2014/2020, Linea di Azione 1.1.1 e 1.1.4, Avviso Pubblico per “Sostegno a progetti di Ricerca Industriale, Sviluppo Sperimentale e Innovazione delle PMI nelle aree di specializzazione S3” (CUP: C37H18000070007).
Authors acknowledge also Roboze s.p.a. for the materials.

References

[1] Singh V, Sharma SK. Fuel consumption optimization in air transport: a review, classification, critique, simple meta-analysis, and future research implications. Eur Transp Res Rev 2015;7:1–24.

[2] Vita A, Castorani V, Germani M, Marconi M. Comparative life cycle assessment of low-pressure RTM, compression RTM and high-pressure RTM manufacturing processes to produce CFRP car hoods. Procedia CIRP 2019;80:352–7.

[3] De Sanctis AM, Evangelista E, Forcellese A, Wang YZ. Hot formability studies on 359/SiC/20p and their application in forging optimisation. Appl Compos Mater 1996;3:179–98.

[4] Roberts SM, Kusiak J, Liu YL, Forcellese A, Withers PJ. Prediction of damage evolution in forged aluminium metal matrix composites using a neural network approach. J Mater Process Technol 1998;80–81:507–12.

[5] A. Forcellese, L. Greco, M. Pieralisi, M. Simoncini GT. Mechanical properties of carbon fiber reinforced plastic obtained by the automated deposition of an innovative towpreg. Accept Publ Procedia CIRP 2020 2020.

[6] Postacchini L, Simoncini M, Forcellese A, Bevilacqua M, Ciarapica FE, Andreassi G, et al. Environmental assessment of an automated impregnation process of carbon fiber tows. Procedia CIRP 2020;88:445-50.

[7] Landi D, Vita A, Borriello S, Scafà M, Germani M. A methodological approach for the design of composite tanks produced by filament winding. Comput Aided Des Appl 2020;17:1229–40.

[8] Ashcroft IA, Hughes DJ, Shaw SJ. Adhesive bonding of fibre reinforced polymer composite materials. Assem Autom 2006;20:150–61.

[9] D'Orazio A, Mehtedi M El, Forcellese A, Nardinocchi A, Simoncini M. Study of tapping process of carbon fiber reinforced plastic composites/AA7075 stacks. AIP Conf. Proc. 2018;1960.

[10] D'Orazio A, El Mehtedi M, Forcellese A, Nardinocchi A, Simoncini M. Tool wear and hole quality in drilling of CFRP/AA7075 stacks with DLC and nanocomposite TiAlN coated tools. J Manuf Process 2017;30:582–92.

[11] Xu Y, Zhang H, Šavija B, Chaves Figueiredo S, Schlangen E. Deformation and fracture of 3D printed disordered lattice materials: Experiments and modeling. Mater Des 2019;162:143–53.

[12] Huybrechts SM, Hahn SE, Meink TE. Grid Stiffened Structures: a Survey of Fabrication, Analysis and Design Methods. Proc. 12th Int. Conf. Compos. Mater. 1999:1.

[13] Wang D, Abdalla MM. Global and local buckling analysis of grid-stiffened composite panels. Compos Struct 2015;119:767–76.

[14] Li W, Sun F, Wang P, Fan H, Fang D. A novel carbon fiber reinforced lattice truss sandwich cylinder: Fabrication and experiments. Compos Part A Appl Sci Manuf 2016;81:313–22.

[15] Hao M, Hu Y, Wang B, Liu S. Mechanical behavior of natural fiber-based isogrid lattice cylinder. Compos Struct 2017;176:117–23.

[16] Zheng Q, Jiang D, Huang C, Shang X, Ju S. Analysis of failure loads and optimal design of composite lattice cylinder under axial compression. Compos Struct 2015;131:885–94.

[17] Chen L, Fan H, Sun F, Zhao L, Fang D. Improved manufacturing method and mechanical performances of carbon fiber reinforced lattice-core sandwich cylinder. Thin-Walled Struct 2013;68:75–84.

[18] Totaro G. Optimal design concepts for flat isogrid and anisogrid lattice panels longitudinally compressed. Compos Struct 2015;129:101–10.

[19] Shroff S, Acar E, Kassapoglou C. Design, analysis, fabrication, and testing of composite grid-stiffened panels for aircraft structures. Thin-Walled Struct 2017;119:235–46.

[20] Wang X, Jiang M, Zhou Z, Gou J, Hui D. 3D printing of polymer matrix composites: A review and prospective. Compos Part B Eng 2017;110:442–58.

[21] Forcellese A, di Pompeo V, Simoncini M, Vita A. Manufacturing of isogrid composite structures by 3D printing. Procedia Manuf., vol. 47, 2020, p. 1096–100.

[22] Li M, Lai C, Zheng Q, Han B, Wu H, Fan H. Design and mechanical properties of hierarchical isogrid structures validated by 3D printing technique. Mater Des 2019;168.